ELSEVIER

Microelectronic Engineering 51–52 (2000) 189–194

MICROELECTRONIC ENGINEERING

www.elsevier.nl/locate/mee

Nonthermal carrier dynamics in $Al_xGa_{1-x}As/GaAs$ quantum wells

K.W. Sun[a,*], T.S. Song[a], S.Y. Wang[b], C.P. Lee[b]

[a]*Department of Electronic Engineering, Feng Chia University, Taichung, Taiwan 407*

[b]*Department of Electronics Engineering and Institute of Electronics, National Chiao Tung University, Hsin Chu, Taiwan*

Abstract

We present new time-resolved measurements that demonstrate the effect of injected carrier densities on carrier–carrier scattering rates of highly nonequilibrium carrier distributions in the p-doped $Al_{0.32}Ga_{0.68}As/GaAs$ quantum wells with well width of 5 and 3 nm. The spectra at high densities ($\geq 10^{10}$ cm^{-2}) demonstrate that the initially narrow electron distribution is altered in a time less than or equal to the LO phonon emission time as the result of rapid carrier–carrier scattering. At about the same excitation density ($\sim 10^{10}$ cm^{-2}), the carrier–carrier scattering rate is faster in 3 nm quantum wells in comparison to 5 nm wells. Our results also indicate that carrier–carrier scattering becomes as significant as LO phonon emission at density of about 1×10^{10} cm^{-2} in the 5 nm quantum wells.

Keywords: Carrier–carrier scattering; LO phonon emission; Nonthermal carrier distributions

The behavior of non-equilibrium carriers in semiconductors is a subject of fundamental interest and technological importance. In reduced dimensionality systems, the effect of quantum confinement on non-equilibrium carriers holds research interest. Recently, femtosecond optical spectroscopy has proven to be an excellent tool for the study of fundamental non-equilibrium properties in semiconductors [1–6]. While there are still questions remaining, it appears safe to say that hot electron relaxation in bulk GaAs is becoming relatively well understood. However, in 2D the situation is quite murky. Less experimental data on carrier–carrier scattering rates are available for 2D carriers than 3D carriers. Kash has studied the energy loss rate of a hot electron to a thermalized electron–hole plasma in $Al_xGa_{1-x}As/GaAs$ quantum wells [7]. The experimental situation of nonthermal carrier distributions in 2D has been dominated by four experiments of Knox et al. [4,8].

In this report we have made a time-resolved measurement of the distribution at the densities below 10^{10} cm^{-2}. We excited the sample with an ultrafast optical pulse and measure the time-integrated hot electron–neutral acceptor (hot(e,Å)) luminescence spectra as a function of photoexcited carrier densities. We are not only able to inject a moderate density of carriers into the sample but also able to create a highly nonequilibrium distribution of hot carriers with our 120 and 180 fs duration pulses because LO phonon emission by the photoexcited carrier is not large during the laser pulses. By

*Corresponding author. Tel.: +886-4-451-7250, ext. 3877; fax: +886-4-451-0405.
E-mail address: kwsun@fcu.edu.tw (K.W. Sun)

0167-9317/00/$ – see front matter
PII: S0167-9317(99)00475-X

measuring the first unrelaxed peak in the hot(e,Å) luminescence spectra, we are assured of sampling the hot electron distribution within an LO phonon emission time (~150 fs) [9–14].

The MQW samples studied here were 5 and 3 nm GaAs wells, both with $x = 0.32$ $Al_xGa_{1-x}As$ barrier of 25 nm thickness. The quantum wells were doped with Be in the central 1 nm of each well to 10^{18} cm^{-3}. The quantum well samples consisted of a stack of 40 wells and were grown on [100] undoped GaAs substrates. For all experiments reported here, the samples were held in a closed-cycled cryostat refrigerator at $T = 10$ K to ensure that virtually all the acceptors are neutral and to reduce the occupancy of LO phonon to insignificant levels. Hot(e,Å) luminescence spectra are taken with the combination of a triplemate spectrometer and a liquid nitrogen cooled CCD detector. The experiments have employed three excitation sources – an argon ion laser pumped CW dye laser, a self-mode-locked Ti:sapphire laser and a mode-locked dye laser. The CW dye laser was operated at energies of 1.797(1.893) eV for the 5(3) nm wells. The self-mode-locked Ti:sapphire laser which generated optical pulses as short as 120 fs was operated at the energy of 1.797 eV with an 80 MHz repetition rate. The mode-locked dye laser is capable of producing 180 fs pulses and is operated at the energy of 1.893 eV with 100 MHz repetition rate.

Fig. 1 shows the time-integrated luminescence spectrum of the 5 nm quantum wells with the CW dye laser used as the excitation source. In Fig. 1, the 'unrelaxed peak' in the spectrum is due to the initial unrelaxed hot electrons excited from the lowest heavy hole band recombining with neutral acceptors. The energy of electrons that have been promoted from the lowest heavy hole valence band and have lost one LO phonon energy coincided with the energy of unrelaxed electrons promoted from the first excited light hole valence band, so that the appearance of the first LO phonon peak was masked.

In Fig. 2 we show spectra of the 5 nm quantum wells obtained with the self-mode-locked Ti:sapphire laser as the excitation source. By defocusing the laser, the injected carrier density can be varied; the photoexcited carrier densities are determined from the laser spot size on the sample and the absorption coefficient of the QW samples at the excitation wavelength. Our detection system is adjusted to sample only the center half of the laser spot, thus minimizing uncertainties associated with

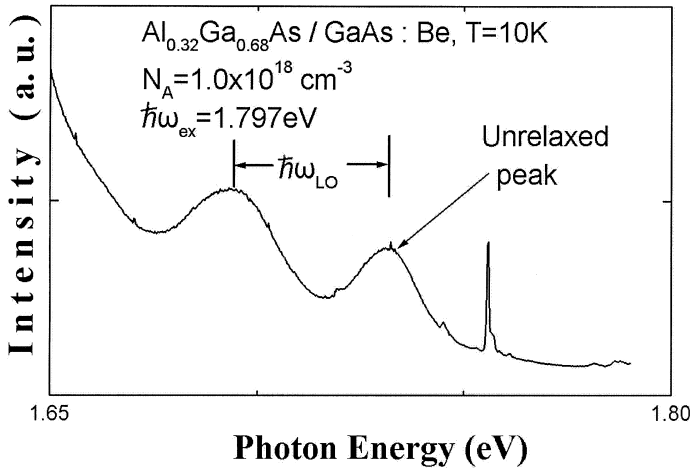

Fig. 1. Time-integrated luminescence of 5 nm quantum wells after CW excitation at 1.797 eV.

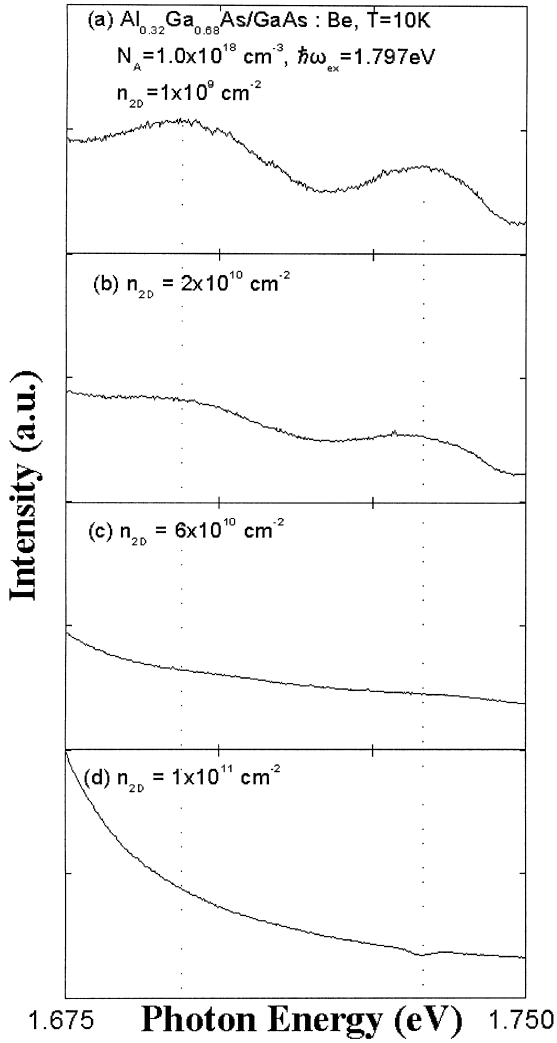

Fig. 2. Time-integrated luminescence of 5 nm quantum wells after femtosecond excitation at 1.797 eV for four injected carrier densities (a) 1×10^{9} cm^{-2}, (b) 2×10^{10} cm^{-2}, (c) 6×10^{10} cm^{-2}, (d) 1×10^{11} cm^{-2}.

non-uniform injection. Injected carrier densities from 1×10^{9} cm^{-2} to 2×10^{11} cm^{-2} are obtained by using the mode-locked Ti:sapphire laser as the excitation source and varying the spot size. The corresponding spectra are shown in Fig. 2a–d. The unrelaxed peaks begin to decrease at a carrier density of 1×10^{9} cm^{-2}. As the injected carrier density is increased toward 1×10^{11} cm^{-2}, the peaks disappear. The height of the unrelaxed peak measures the density of electrons at the initial energy convolved with broadening mechanism such as acceptor–acceptor interactions. We find no change in the linewidth of the peak, and thus measurements of the integrated area under the peak give the same results as measuring the peak height. In Fig. 3 we plot the unrelaxed peak intensity relative to the background (which remain relatively constant) in each spectrum as a function of injected carrier density. The probability is small that an electron will be scattered out of this peak before emitting an

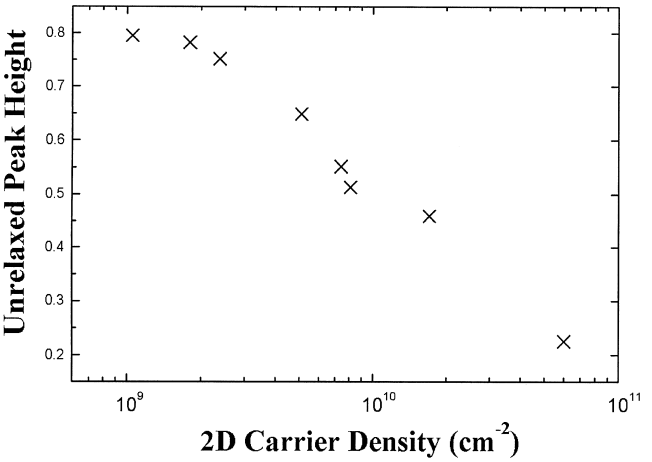

Fig. 3. The unrelaxed peak intensities (relative to the background) in each spectrum taken in the Ti:sapphire laser experiments are plotted as the function of injected carrier densities.

LO phonon if, during an LO phonon emission time, scattering transfers little energy among carriers relative to the width of the peak. Thus at low densities the unrelaxed peak is unaffected by carrier–carrier scattering. At higher densities, however, the interactions among carriers are stronger, and at sufficiently high densities carrier–carrier scattering will reduce the height of the unrelaxed peak. The height of the unrelaxed peak thus allowed us to compare the relative importance of carrier–carrier scattering and LO phonon emission for the scattering of energetic electrons. We interpret the decrease of the unrelaxed peak as the injected carrier density is increased as evidence that carrier–carrier scattering is becoming important [15,16]. By interpolation, we find that at an injected carrier density of 1×10^{10} cm^{-2} the intensity drops by a factor of two compared to the CW experiment. Thus the crossover from scattering dominated by LO phonon emission to scattering dominated by the carrier–carrier interaction occurs at about this density.

Fig. 4a and b show the time-integrated hot(e,Å) luminescence spectrum of the 3 nm quantum wells with the CW and mode-locked dye lasers used as the excitation sources. We have used excitation sources operated at appropriate photon energies in order to give approximately the same amount of excess kinetic energy to the photoexcited carriers as in the 5 nm quantum well experiments. In Fig. 4a we can clearly see that the electrons have relaxed through successive LO phonon emission events before recombining with neutral acceptors as in the 5 nm quantum wells experiments excited with a CW dye laser. In Fig. 4b we show the spectrum obtained with the mode-locked dye laser as the excitation source. However, even at excitation density as low as 10^{10} cm^{-2}, we still observed a featureless spectrum. The absence of any structures with LO phonon spacing in Fig. 4b not only indicates that inelastic carrier–carrier scattering is the dominant mechanism of thermalization but the inelastic scattering rates are also much faster than 5 nm quantum well experiments at about the same density. We attribute this to the stronger quantum confinement and weaker screening in narrower quantum wells.

Calculations of 2D carrier–carrier scattering have not yet explored the dependence of scattering on relevant parameters such as the carrier density. Most of the previous calculations of 2D carrier–carrier

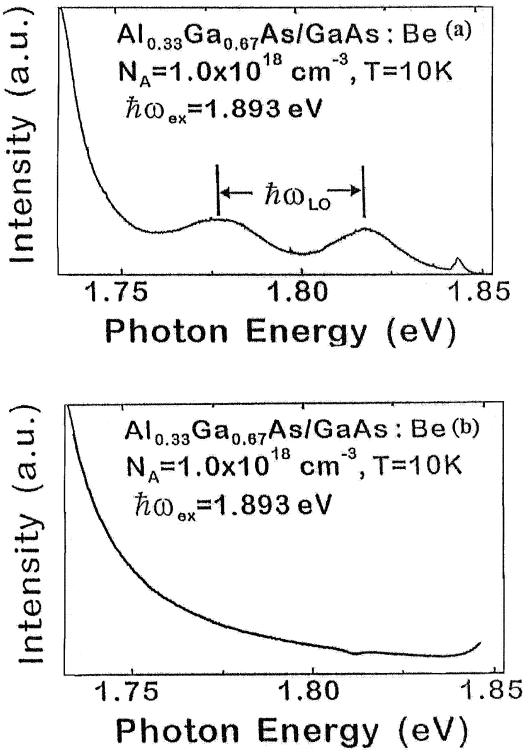

Fig. 4. Time-integrated luminescence of 3 nm quantum wells after CW (a) and femtosecond (b) excitation at 1.893 eV. The injected carrier density in spectra (b) is at about 1×10^{10} cm^{-2}.

scattering have used a static screening model except the Monte Carlo study by El-Sayed et al. [17] and Kane's work [18] by solving the dynamically screened Boltzmann equation. Our results are in qualitative agreement with Kane's theoretical works in which he has studied the carrier–carrier scattering using integration of the dynamically screened Boltzmann equation. In his studies, 2D electron–hole pairs are generated in GaAs quantum wells with an average energy of 20 meV, and an average hole energy of 12 meV. The initial energy width (FWHM) of the electron peak is 20 meV. The evolution of the electron distribution is followed for 150 fs. The initial electron peak height dropped by a factor of two as the density was increased to 5×10^{10} cm^{-2}. In our experiments, by interpolation, we find that at an injected carrier density of 1×10^{10} cm^{-2} the intensity drops by a factor of two compared to the CW experiment. The slight difference between the experimental results and calculations is probably due to the higher electron excess energy for the photoexcited carriers in our experiments. To our knowledge there is no dynamically screened calculations on dependence of the quantum well width for 2D carrier–carrier scattering.

In conclusion, our experimental results show that at an injected density lower than 1×10^{10} cm^{-2} the hot electrons lose their energy to the lattice before appreciable attenuation by carrier–carrier scattering. As the carrier density is increased from 1×10^{9} cm^{-2} to 2×10^{11} cm^{-2}, however, the carrier–carrier scattering begins to compete with carrier–phonon scattering, with a crossover in their relative importance at $\sim 1 \times 10^{10}$ cm^{-2}. At carrier densities greater than 1×10^{11} cm^{-2}, carrier–

carrier scattering is the dominant scattering process. We also find that, at about the same injected carrier density, carrier–carrier scattering rate is faster in 3 nm wells than in 5 nm wells.

Acknowledgements

This work was supported by the National Science Council of Republic of China under contract Grant no. NSC87-2112-M-035-004 and NSC86-2112-M-035-008.

References

[1] D.W. Snoke, W.W. Ruhle, Y.C. Lu, E. Bauser, Phys. Rev. Lett. 68 (1992) 990.
[2] D.W. Snoke, W.W. Ruhle, Y.C. Lu, E. Bauser, Phys. Rev. B45 (1992) 10979.
[3] A. Leitenstorfer, C. Furst et al., Phys. Rev. Lett. 76 (1996) 1545.
[4] W. Knox, C. Hirlimann, D.A.B. Miller, J. Shah, D.S. Chemla, C.V. Shank, Phys. Rev. Lett. 56 (1986) 1191.
[5] T. Elsaesser, J. Shah, L. Rota, P. Lugli, Phys. Rev. Lett. 66 (1991) 1757.
[6] J. Shah, B. Deveaud, T.C. Damen, W.T. Tsang, A.C. Gossard, P. Lugli, Phys. Rev. Lett. 59 (1987) 2222.
[7] J.A. Kash, Phys. Rev. B48 (1993) 18336.
[8] W.H. Knox, D.S. Chemla, G. Livescu, J.E. Cunningham, J.E. Henry, Phys. Rev. Lett. 61 (1988) 1290.
[9] B.P. Zakharchenya, P.S. Kop'ev, D.N. Mirlin, D.G. Polakov, I.I. Reshina, V.F. Sapega, A.A. Sirenko, Solid State Commun. 69 (1989) 203.
[10] C.V. Shank, R.L. Fork, R. Yen, J. Shah, B.I. Greene, A.C. Gossard, C. Weisbuch, Solid State Commun. 47 (1983) 981.
[11] J. Shah, IEEE J. Quantum Electron. QE-22 (1986) 1728.
[12] S.A. Lyon, Superlattice Microstruct. 3 (1987) 261.
[13] D.N. Mirlin, V.I. Perel, Semicond. Sci. Technol. 7 (1992) 1221.
[14] D. Collings, K.L. Schumacher, F. Raksi, H.P. Hughes, R.T. Philips, Appl. Phys. Lett. 64 (1994) 889.
[15] K.W. Sun, M.G. Kane, S.A. Lyon, Europhys. Lett. 26 (1994) 123.
[16] A. Leitenstorfer, T. Elsaesser, F. Rossi, T. Kuhn, W. Klien, G. Boehm, G. Traenkle, G. Weimann, Phys. Rev. B53 (1996) 9876.
[17] K. El Sayed, H. Haug, Phys. Status Solidi B173 (1992) 189.
[18] M.G. Kane, Phys. Rev. B54 (1996) 16345.